NON-SYNCRHONOUS WHIRLING DUE TO FLUID-DYNAMIC FORCES IN AXIAL TURBO-MACHINERY ROTORS

Shan Fu Shen and Vinod G. Mengle
Cornell University
Ithaca, New York 14853

SUMMARY

The role of fluid-forces acting on the blades of an axial turbo-rotor with regards to whirling is analyzed. The dynamic equations are formulated for the coning mode of an overhung rotor. The exciting forces due to the motion are defined through a set of "rotor stability derivatives" (R.S.D.'s), and analytical expressions of the aerodynamic contributions are found for the case of small mean stream deflection, high-solidity and equivalent flat plate cascade. (Torque-whirl and tip-clearance effects can also be included in the R.S.D.s). For a typical case, only backward whirl is indicated if the phase-shifting of the rotor wake effect is ignored. A parametric study of the dynamic stability boundary reveals that a reduction in blade stagger angle, mass-flow rate, fluid density and an increase in stiffness and external damping are all inducive for improved stability. An optimum overhang distance of the rotor from the bearing-support can also be found. Finally, when two or more opposing whirling mechanisms are present, mutual annihilation is possible by making a certain whirling group "b_o" very small. This concept can be useful in the preliminary design stage or for later improvements.

INTRODUCTION

An increasing number of severe failures in high speed compressors and turbines in recent years are attributable to whirling instability. Ehrich (ref. 1), Shapiro and Colsher (ref. 2) and many others have reviewed the destabilizing mechanisms. To our knowledge, only a few studies have been conducted regarding the fluid-dynamic forces acting on the blades themselves. Alford (ref. 3) dealt only with the periphery of the rotor, namely, the tip-clearance and labyrinth seal forces. Reference 4 includes various other mechanisms acting between the rotor-circumference and its casing. Bousso (ref. 5) and later Vance (ref. 6) analyzed the consequences of the tilting of load-torque, but did not account for other effects produced by the same fluid forces. Trent and Lull (ref. 7) noted the important analogy between turbo-rotor whirl and propeller whirl. Ehrich (ref. 8) considered the fluid reactions based on Euler's turbine equations but his dynamic equation was later found to be in error.

In this paper, we adopt the usual modelling of an overhung rotor in its 'coning mode' to set up the dynamic equations of motion. The forcing terms are from the self-induced aerodynamic forces due to the motion, and the whirling is

thus reduced to an eigenvalue problem much like flutter. The analysis follows the basic idea of propeller whirl but the details are carefully reworked for the cascade configuration in turbo-rotor systems. Our emphasis is to lay down a proper framework and outline the methodology, so that only systematic refinements and extensions are needed to yield results of practical significance.

SYMBOLS

a_1, b_1 displacements of shaft-center in y- and z-directions respectively

$\underline{\underline{C}}$ diagonal damping matrix with elements $c_d e^2$

C complex wake function

C_ℓ coefficient of lift

C_{α_β} Rotor Stability Derivative (R.S.D.)

c chord length

$D = 2\zeta K_\theta (e/r_2')^2$

e equivalent overhang shaft length

F real part of wake function C

G imaginary part of wake function C

$H =$ J/I, ratio of inertias

$\underline{\underline{I}}$ diagonal inertia matrix with elements I

$I = Mr_2'^2$, moment of inertia of rotor about pivotal axis

$\hat{i}, \hat{j}$ unit vectors in axial flow direction and opposite to rotational speed, respectively

J polar moment of inertia of rotor

$\underline{\underline{K}}$ diagonal stiffness matrix with elements K

K, k_1 equivalent torsional spring

k_o cascade interference factor

$K_\theta = \omega_\theta R/V_a$, reduced structural frequency

k reduced aerodynamic frequency

ℓ elemental lift

M mass of rotor

$M' = \pi R^2 \rho V(1 - \eta_o^2)$, annular mass flow rate

m elemental moment

r radial location

r_2' $(r_2^2 + e^2)^{1/2}$, radius of gyration of rotor about pivotal axis

R rotor tip radius

s gap between adjacent chords

T kinetic energy

t time

V potential energy

V absolute velocity

W relative velocity

β angle of velocity component with respect to axial direction

γ blade stagger angle

Δ change

δ angle of attack

$\eta = r/R$

η_o hub-to-tip radius ratio

θ_o amplitude of pitch angle

θ_1 coning angle

θ_i azimuthal location of i th blade from horizontal axis

$\kappa = \pi R^5 \rho(1 - \eta_o^2)/I$, ratio of moment of inertia of annular cylinder of air to that of rotor

ρ fluid density

$\sigma =$ c/s, solidity ratio

ϕ = $V/\Omega R$, tip mass-flow coefficient

ψ_o amplitude of yaw angle

$\underline{\omega}$ angular velocity vector

$\omega_\theta = \sqrt{K/I}$

Subscripts, prefixes, etc.:

o steady value

1,2 inlet and exit stations

1,2 forward and backward whirl

1,2 refers to $(\Omega \pm \omega)$ in context with reduced frequencies for whirl reference value

a axial direction

$( )^a$ aerodynamic contribution

comp compressible

eff effective

inc incompressible

Im imaginary part

Re real part

s inertial reference frame

x,y,z in the direction of x,y,z axes

w wake contribution

θ tangential direction

$\bar{(\ )}$ average value

$(')$ perturbed value

$\underline{\underline{(\ )}}$ matrix notation

THE ROTOR MODEL

A rotor on a flexible shaft is equivalent to a gyroscope tied to a rotating spring. Figure 1 shows the real rotor shaft system and the idealized model considered in this paper. This simplest model focuses on the 'coning mode' and has all the characteristics necessary to produce the phenomenon under study. Some of the implications and further assumptions are:

1. The shaft elastica remains in one plane due to infinite stiffness in torsion.
2. The angular tilt of the rotor axis essential for the coning mode is coupled to the radial deflection of the center of the rotor.
3. The cantilevered shaft is approximated by an equivalent, torsional spring, k_1 and an equivalent, rigid, massless shaft of length, l_1. The notation $K = k_1$ and $e = l_1$ is used in the main text. (See reference 9 for inadequacies in this model.)
4. The bearings are rigid and frictionless.
5. The center of mass of the rigid rotor is at its geometric center, i.e. there is no imbalance or eccentricity.

LAGRANGE'S EQUATIONS OF MOTION

The motion and instantaneous position of the rotor can be completely specified by the Euler angles ψ, θ and Ωt which are, respectively, the yaw, pitch and azimuth angle as shown in figure 2. For small angular deflections ψ, θ and constant rotational speed Ω, we have

$$\omega_x \cong \Omega + \dot{\psi}\theta \ , \quad \omega_y \cong -\dot{\theta} \quad \text{and} \quad \omega_z \cong \dot{\psi} \tag{1}$$

The dynamic equations are derived by using Lagrange's equations:

$$\frac{d}{dt}\left(\frac{\partial L}{\partial \dot{q}_i}\right) - \frac{\partial L}{\partial q_i} + \frac{\partial D}{\partial \dot{q}_i} = Q_i \tag{2}$$

where,

L = Lagrange function = $T - V = \frac{1}{2}\,\underline{\omega}^T \cdot \underline{\underline{I}} \cdot \underline{\omega} - \frac{1}{2}\,\underline{q}^T \cdot \underline{\underline{K}} \cdot \underline{q}$

D = Dissipation function = $\frac{1}{2}\,\dot{\underline{q}}^T \cdot \underline{\underline{C}} \cdot \dot{\underline{q}}$

Q_i = Generalized force = $\delta W/\delta q_i$

δW = Virtual work

and q_i = Generalized degree of freedom (d.o.f.); ($q_1 = \psi$, $q_2 = \theta$)

After simplifications, the results may be written as:

$$\begin{Bmatrix} I & 0 \\ 0 & I \end{Bmatrix} \begin{Bmatrix} \ddot{\psi} \\ \ddot{\theta} \end{Bmatrix} + \begin{Bmatrix} c_d e^2 & J\Omega \\ -J\Omega & c_d e^2 \end{Bmatrix} \begin{Bmatrix} \dot{\psi} \\ \dot{\theta} \end{Bmatrix} + \begin{Bmatrix} K & 0 \\ 0 & K \end{Bmatrix} \begin{Bmatrix} \psi \\ \theta \end{Bmatrix} = \begin{Bmatrix} Q_1 \\ Q_2 \end{Bmatrix} \tag{3}$$

In particular, note that I is the moment of inertia of the rotor about the "pivotal axis" and c_d is the "equivalent viscous damping coefficient" to account for the damping effects assumed to be representable by an effective force applied at the tip of the shaft.

According to the principle of virtual work, $\delta W = M_z\,\delta\psi + M_y\,\delta\theta$. It follows that $Q_1 = M_z$ and $Q_2 = M_y$, i.e. the generalized forces are the pivotal moments M_z and M_y produced due to the fluid-dynamic forces acting on the rotor. These moments are found in the next section to be functions of both the generalized d.o.f., q_i, and their derivatives. Thus, besides the anti-symmetric gyroscopic coupling due to $\pm J\Omega$ there also exists coupling due to the fluid-dynamic forces. Such external couplings, if anti-symmetric in nature, as is well known, can produce unstable response.

THE ROTOR STABILITY DERIVATIVES (R.S.D.'s)

The generalized forces caused by small perturbations of the d.o.f. will be expressed as a set of 'rotor stability derivatives', abbreviated as R.S.D.'s, in this paper. For a systematic treatment of the aerodynamic terms, the analogy of the present problem to propeller whirl treated in References 10 and 11 is obvious. However, we have to make judicial adjustments for the cascade configurations. As a first approximation, we consider here only the quasi-steady effect of inviscid, potential fluid flow on an axial turbo-compressor.

The quasi-steady lift for an airfoil in cascade depends on the instantaneous angle of attack and is given by

$$\ell = \frac{1}{2}\,\rho W_{eff}^2\, C_{\ell_{eff}}\, c\, \Delta r \quad . \tag{4}$$

In order to find the effective reference velocity, W_{eff}, and the coefficient of lift $C_{\ell_{eff}}$, consider the displaced rotor as shown in figure 3a. A circumferential cut AA at any radial location unfolds a cascade of airfoils which can be represented simply by equivalent flat plates as shown in figure 3b (see ref. 12). It is well known that, for a cascade of high solidity, i.e. small gap-to-chord ratio ($s/c \lesssim 0.7$), the angle of the relative outlet velocity with respect to the blade is independent of the relative inlet flow angle and is equal to the equivalent flat plate stagger angle. Hence, assuming that the rotation of the blade due to yaw and pitch is very small as compared to its stagger angle, γ, the perturbed and steady relative outlet velocities, $\vec{W}_2'$ and $\vec{W}_2$, are approximately parallel to each other. Next, assuming constant radius cylindrical stream surfaces, the equation of continuity gives the equivalence of the axial components of the absolute outlet velocity in the steady and perturbed states, i.e. $V'_{a2} = V_{a2} = V_a$. The velocity triangles in figure 3c are shown using these assumptions. The velocity triangles are crucial to the development of the R.S.D.'s. (See ref. 9 for further discussions.)

Defining the reference velocity in cascades by

$$\vec{W}_\infty \equiv \frac{1}{2}(\vec{W}_1 + \vec{W}_2) \tag{5}$$

we get

$$\Delta\vec{W}_\infty \equiv \vec{W}'_\infty - \vec{W}_\infty = v\hat{i} + \frac{1}{2}(u + v\tan\beta_2)\hat{j} \tag{6}$$

where, u and v are the perturbation velocities of the blade in the plane of the rotor disc and normal to it. From kinematical relationships, we can easily write

$$u = -e\dot{\psi}\sin\Omega t + e\,\dot{\theta}\cos\Omega t$$

$$v = (\psi\Omega - \dot{\theta})\,r\sin\Omega t - (\theta\Omega + \dot{\psi})\,r\cos\Omega t \tag{7}$$

The angular tilt of the rotor axis and the component of $\Delta\vec{W}_\infty$ normal to $\vec{W}_\infty$ combine to give an effective change in the angle of attack,

$$\Delta\delta = \delta_1 + \delta_2 \tag{8}$$

where,

$$\delta_1 = \psi\sin\Omega t - \theta\cos\Omega t$$

$$\delta_2 = -v\,(\Omega r + V_a\tan\beta_2 - V_{\theta 1})/2W_\infty^2 + \frac{1}{2}(u + v\tan\beta_2)(V_a/W_\infty^2)$$

Using the coefficient of lift for a flat-plate cascade (ref. 11)

$$C_{\ell_{eff}} = 2\pi\, k_o \sin\delta_{eff} \tag{9}$$

with $\delta_{eff} = \delta_o + \Delta\delta$

and putting $W_{eff} = W_\infty + \Delta W$

where ΔW = component of $\Delta\vec{W}_\infty$ parallel to $\vec{W}_\infty$,

we get the perturbed component of lift from equation (4) as follows:

$$\frac{\ell'}{\pi\rho k_o c\,\Delta r} = W_\infty^2 \cos\delta_o\,\Delta\delta + 2\,W_\infty \sin\delta_o\,\Delta W + 2W_\infty \cos\delta_o\,\Delta W\,\Delta\delta + \sin\delta_o\,\Delta W^2 + \Delta W^2\,\Delta\delta. \tag{10}$$

The first term provides the leading contribution and for lifting cascades (i.e. $\delta_o \neq 0$) the second term gives an additional small effect. Equation (10) is a general expression for the perturbed lift component; it can be written for the i th blade by replacing Ωt by $\Omega t + \theta_i$, then summed over all the blades and finally integrated from the hub to the tip radius giving the total perturbed lift.

We now specialize equation (10) for a non-lifting cascade, i.e. $\delta_o = 0$ and uniform axial inlet field with no swirl, i.e. $V_{\theta 1} = 0$. It turns out that even in such a simple case significant forces may be produced.

Using the simple relation for the cascade interference factor, k_o

$$k_o = \frac{2}{\pi}\,\frac{s}{c}\,\frac{1}{\cos\gamma} \tag{11}$$

for a high solidity cascade with $(s/c) \lesssim 0.7$, (see ref. 12), the following result for the non-dimensional force components can be obtained:

$$\frac{P_y}{M'V_a} = C_{y_\psi}\,\psi + C_{y_q}\left(\frac{\dot\psi\,R}{V_a}\right) + C_{y_r}\left(\frac{\dot\theta\,R}{V_a}\right)$$

$$\frac{P_z}{M'V_a} = C_{z_\theta}\,\theta + C_{z_r}\left(\frac{\dot\theta\,R}{V_a}\right) + C_{z_q}\left(\frac{\dot\psi\,R}{V_a}\right) \tag{12}$$

where

$$C_{y_\psi} = C_{z_\theta} = 1 + (1 + \eta_o^2)/(4\phi^2)$$

$$C_{y_q} = C_{z_r} = -\,e/2R$$

$$C_{y_r} = -C_{z_q} = (1 + \eta_o^2)/(4\phi^2)\ . \tag{13}$$

Similarly, integrating the elementary moment components

$$m_y = -\,r\,\ell_y \tan\beta_\infty$$

and

$$m_z = r\,\ell_z \tan\beta_\infty \tag{14}$$

we get the non-dimensional moment components as

$$\frac{M_y^a}{M'V_a R} = C_{m_\psi}\,\psi + C_{m_q}\left(\frac{\dot{\psi} R}{V_a}\right) + C_{m_r}\left(\frac{\dot{\theta} R}{V_a}\right)$$

$$\frac{M_z^a}{M'V_a R} = C_{n_\theta}\,\theta + C_{n_r}\left(\frac{\dot{\theta} R}{V_a}\right) + C_{n_q}\left(\frac{\dot{\psi} R}{V_a}\right) \qquad (15)$$

where

$$C_{m_\psi} = -C_{n_\theta} = -\left[(1 + \eta_o^2)/2\phi + (1 + \eta_o^2 + \eta_o^4)/6\phi^3\right]$$

$$C_{m_q} = -C_{n_r} = \frac{1}{4}\frac{e}{R}(1 + \eta_o^2)/\phi$$

$$C_{m_r} = C_{n_q} = -(1 + \eta_o^2 + \eta_o^4)/6\phi^2 \; . \qquad (16)$$

Analogous to the propeller-in-yaw studies, for example, by Ribner (ref. 13) the perturbed axial force and torque about the rotor axis are zero.

The coefficients C_{y_ψ}, C_{y_q}, C_{y_r}, C_{m_ψ}, C_{m_q}, C_{m_r}, etc. as defined by equations (12-16) and which denote increases in forces/moments due to unit increases in the d.o.f. or their derivatives are termed as the 'Rotor Stability Derivatives' in this paper. Note that in this formulation the R.S.D.'s are independent of the number of blades and solidity ratio and remind one of actuator disc type results. In practical applications reliable determination of the R.S.D.'s is, of course, imperative.

APPROXIMATE CORRECTIONS FOR COMPRESSIBILITY AND WAKE EFFECTS

For compressible flows, a first-order correction on the pressure distribution can be obtained by using the expression given in reference 12, page 61. For the case of small lift and low subsonic Mach numbers it reduces to the well-known Prandtl-Glauert Rule:

$$(C_\ell)_{comp} = (C_\ell)_{inc} \Big/ \sqrt{1 - M_\eta^2}$$

where M_η is the local Mach number at any radial location η. The concept of an effective Mach number, M_{eff} was used by Ribner (ref. 13) as an overall correction to the R.S.D. So long as M_{eff} is small, we find only small changes in the R.S.D.'s and the stability boundaries are not significantly affected.

The unsteady rotor wake can be taken into account by the use of complex rotor wake functions; see Houbolt and Reed (ref. 10) in the propeller whirl problem. Instead of the well known Theodorsen function for an isolated airfoil, one needs the oscillating cascade wake functions, C, for example, by Whitehead (ref. 14). In cascades the wake function is a parameter of not only the reduced frequency, k, but also of solidity, blade stagger angle and the phase of vibration between adjacent blades, Φ. Hence,

$$F \equiv \text{Re}\{C\} = \text{fn}\,(k, s/c, \gamma, \Phi)$$

and

$$G \equiv \text{Im}\{C\} = \text{fn}\,(k, s/c, \gamma, \Phi) \quad . \tag{17}$$

Analysis done parallel to reference 10 leads to the following important conclusions for multi-bladed cascaded rotors (see ref. 9):

1. Two reduced frequencies are involved in whirling:

$$k_{1,2} = (\Omega \pm \omega)\, c/2W_\infty \tag{18}$$

2. If the whirling frequency ω is much smaller than the rotor frequency Ω, then the effect of wake is to turn the resultant force and moment clockwise by approximately:

$$\delta^* = \tan^{-1}\,(\bar{G}/\bar{F}) \tag{19}$$

where

$$\bar{F} = \frac{1}{2}\left\{F(k_1) + F(k_2)\right\}$$

$$\bar{G} = \frac{1}{2}\left\{G(k_1) + G(k_2)\right\} \tag{20}$$

without much change in the magnitude of the vectors.

3. Two new R.S.D.'s solely attributable to this effect are added, namely,

$$C^w_{y_\theta} = -C^w_{z_\psi} \cong C_{y_\psi} \tan\delta^*$$

$$C^w_{m_\theta} = C^w_{n_\psi} \cong C_{m_\psi} \tan\delta^* \quad . \tag{21}$$

Hence, the contribution to the effective tangential force due to the angular tilt of the rotor, which is important for whirl, appears from two sources:

i) C_{m_ψ} : the quasi-steady moment R.S.D.

ii) $C^w_{z_\psi}$: the unsteady rotor wake force R.S.D.

Ehrich's analysis (ref. 8) did not include either of the above two mechanisms.

The above analysis which was for a compressor or a negative work turbo-machine can be repeated for a turbine or a positive work turbo-machine. Though the previously derived R.S.D.'s are not applicable for thick, curved turbine blades with high flow deflection, it can be shown that the direction of the net force and moment does not change.

For lifting rotors, two other important mechanisms discussed in the literature are Alford's tip-clearance effect (ref. 3) and Bousso's torque whirl effect (ref. 5). Both can be represented by an equivalent tangential force due

to a radial displacement and contribute thus only to C_{z_ψ} (= $-C_{y_\theta}$). In ref. 9 the conversion to R.S.D. is explicitly given.

DYNAMIC STABILITY ANALYSIS

The generalized forces are related to the fluid-dynamic forces and moments by

$$Q_1 = M_z = eP_y + M_z^a$$
$$Q_2 = M_y = eP_z + M_y^a \quad . \tag{22}$$

It is advantageous to write the equation of motion (eqn. (3)) in non-dimensional form. Defining a new independent variable

$$\tau = V_a t/R \tag{23}$$

and denoting derivatives with respect to τ as superscripted primes,

$$\begin{Bmatrix} 1 & 0 \\ 0 & 1 \end{Bmatrix} \begin{Bmatrix} \psi'' \\ \theta'' \end{Bmatrix} + \begin{Bmatrix} D & H/\phi \\ -H/\phi & D \end{Bmatrix} \begin{Bmatrix} \psi' \\ \theta' \end{Bmatrix} + \begin{Bmatrix} K_\theta^2 & 0 \\ 0 & K_\theta^2 \end{Bmatrix} \begin{Bmatrix} \psi \\ \theta \end{Bmatrix} = \kappa \begin{Bmatrix} f_\psi \\ f_\theta \end{Bmatrix} \tag{24}$$

where the non-dimensional forces are given by

$$f_\psi = a_o \psi + a_1 \psi' + b_o \theta + b_1 \theta'$$
$$f_\theta = a_o \theta + a_1 \theta' - b_o \psi - b_1 \psi' \tag{25}$$

with

$$a_o = \frac{e}{R} C_{y_\psi} + C_{m_\theta}$$
$$a_1 = \frac{e}{R} C_{y_q} + C_{m_r}$$
$$b_o = \frac{e}{R} C_{y_\theta} - C_{m_\psi}$$
$$b_1 = \frac{e}{R} C_{y_r} - C_{m_q} \tag{26}$$

Hence, the homogeneous equation is

$$\begin{Bmatrix} 1 & 0 \\ 0 & 1 \end{Bmatrix} \begin{Bmatrix} \psi'' \\ \theta'' \end{Bmatrix} + \begin{Bmatrix} D-\kappa a_1 & H/\phi-\kappa b_1 \\ -H/\phi+\kappa b_1 & D-\kappa a_1 \end{Bmatrix} \begin{Bmatrix} \psi' \\ \theta' \end{Bmatrix} + \begin{Bmatrix} K_\theta^2-\kappa a_o & -\kappa b_o \\ \kappa b_o & K_\theta^2-\kappa a_o \end{Bmatrix} \begin{Bmatrix} \psi \\ \theta \end{Bmatrix} = \begin{Bmatrix} 0 \\ 0 \end{Bmatrix} \tag{27}$$

The anti-symmetric off-diagonal terms $(H/\phi - \kappa b_1)$ and $(-\kappa b_o)$ are important to the self-excited whirl phenomenon as noted earlier.

In order to find the conditions for which the system becomes neutrally stable, sinusoidal motion for ψ and θ is specified:

$$\psi = \psi_o e^{i\omega t} \quad , \quad \theta = \theta_o e^{i\omega t} \tag{28}$$

where ω, the whirling frequency is assumed positive.

To avoid a frontal attack of the eigenvalue problem with a large number of parameters, the following approach has proved to be more fruitful. Let D in equation (27) be replaced by $\bar{D}$ which denotes the damping required for neutral stability. Then the substitution of equation (28) in equation (27) gives rise to two algebraic equations in terms of the two unknowns ω and $\bar{D}$. Equating the real and imaginary parts to zero gives

$$\lambda^2 = \frac{1}{2K_\theta^2}\left(b \pm \sqrt{b^2 - 4d}\right) \tag{29}$$

and

$$\bar{\zeta} = \frac{\bar{D}}{2K_\theta (e/r_2')^2} = \frac{1}{2K_\theta (e/r_2')^2}\left\{\kappa a_1 + \frac{(H/\phi - \kappa b_1)\kappa b_o}{K_\theta^2(1-\lambda^2) - \kappa a_o}\right\} \tag{30}$$

where $\lambda = \omega/\omega_\theta$, non-dimensional whirling frequency

$\bar{\zeta} = c_d/2M\omega_\theta$, fraction of critical damping required for neutral stability

$$b = (H/\phi)^2 + 2K_\theta^2 - 2\kappa\,(a_o + Hb_1/\phi) + \kappa^2(a_1^2 + b_1^2) - 2\bar{D}\kappa a_1 + \bar{D}^2$$

$$d = (K_\theta^2 - \kappa a_o)^2 + (\kappa b_o)^2 \,. \tag{31}$$

It is necessary for neutral stability that $\lambda^2 \geq 0$. Further, only the positive root for λ is taken and $(b^2 - 4d) \geq 0$ should be satisfied.

The equations (29) and (30) are non-linear in λ and $\bar{\zeta}$; but for the κ- and $\bar{\zeta}$-values of interest, the second order appearance of $\bar{\zeta}$ or $\bar{D}$ in λ^2 can be usually neglected. Letting b* denote the value of b with $\bar{D} = 0$, a very good estimate of λ can be obtained, namely,

$$\lambda_{1,2}^2 = \frac{1}{2K_\theta^2}\left(b^* \pm \sqrt{b^{*2} - 4d}\right) \tag{32}$$

Substitution of these λ_1, λ_2 into equation (30) gives the corresponding $\bar{\zeta}_1$ or $\bar{\zeta}_2$. If the actual damping ζ is larger than the damping required for neutral stability, $\bar{\zeta}$, we conclude the system must be stable. Otherwise, the system is unstable and the amplitude increases unless limited by non-linearities. Examination of $\bar{\zeta}$ (eqn. (30)) reveals that since κa_1, occurring due to aerodynamic damping, is always negative, a 'conservative estimate' of $\bar{\zeta}$ can be obtained by dropping κa_1 term. Further analysis shows that generally the term $(1 - \lambda^2)$ changes sign for the two roots of equation (32). A conservative estimate of the needed $\bar{\zeta}$ is thus proportional to b_o, the whirling group. Hence, the larger the magnitude of b_o the larger is the value of damping required to prevent whirling.

NUMERICAL RESULTS FOR AN EXAMPLE AND DISCUSSION

Table I gives typical values of design parameters used for numerical analysis. They are believed to be representative of small, high-speed turbo-rotors. The high value of the hub-to-tip radius ratio is tailored to approximate our assumption of constant radius cylindrical stream-surfaces.

The R.S.D.'s are shown in figure 4 as functions of the tip-mass flow coefficient, ϕ. Since $\phi = \cos\gamma$, we notice that R.S.D.'s increase with the blade stagger angle. The whirling R.S.D.'s C_{m_ψ} and $C^{w}_{y_\theta}$ (which is proportional to C_{y_ψ}) are relatively larger as compared to the remaining R.S.D.'s. Note that $C^{w}_{y_\theta}$ also depends on tan δ^*, where δ^* is the wake angle given by equation (19). The numerous simplified assumptions under which these R.S.D.'s were formulated constrain them to only a small range of blade stagger angles.

It is instructive to examine the effect of only the gyroscopic coupling $\pm J\Omega$. Thus, neglecting all the external aerodynamic forces and the viscous damping, a plot of λ versus the non-dimensionless rotating speed, Ω/ω_θ, as given by equation (29) is shown in figure 5. At any given rotor speed, the two whirling frequencies λ_1 and λ_2, corresponding to forward and backward whirl, respectively, drift further apart from each other as the parameter H, the ratio of moments of inertias of the rotor is increased. Also, at higher rotor-speeds the backward whirling frequency is very small as compared to the forward one or the rotor speed itself. When a slight damping is present both these modes die out. However, without the fluid-dynamic forces, the gyroscopic action cannot in itself lead to a divergent type whirl instability because the net energy input to the system is zero.

The inclusion of the R.S.D.'s through κ in the whirling frequency expression has an imperceptible effect on λ itself. Hence, the forced whirling frequencies are approximately the same as the natural whirling frequencies. Figure 6 shows λ vs. $1/K_\theta$ with ϕ as parameter. K_θ is the reduced structural frequency and is a convenient independent variable. A tendency to converge to the natural frequency ω_θ is observed as the mass-flow coefficient is increased.

The stability boundary plots $\bar{\zeta}$ vs. $1/K_\theta$ are shown in figure 7 for various parameters. In figure 7a where ϕ is a parameter and wake effects are not included the damping required for forward whirl is negative, i.e. $\bar{\zeta}_1 < 0$. Hence, the quasi-steady analysis predicts no forward whirl. On the other hand, backward whirl can occur and rotors with small ϕ and large $1/K_\theta$ values are more susceptible to whirl. Other studies in ref. 9 indicate that increasing the fluid density or Mach number should decrease stability in general; whereas increasing the rotor-to-bearing distance has a stabilizing effect as in figure 7c. This is attributable to the increase in aerodynamic damping term, κa_1, and also due to the form of the fractional damping ζ assumed. The effect of unsteady rotor wake in terms of the wake angle δ^* is shown in figure 7b. In isolated airfoils the calculation of δ^*, say, from Theodorsen's function always gives negative δ^* for all values of the reduced frequency $0 \leq k < \infty$, and, hence, has a stabilizing effect (ref. 10). In cascades, the cascade Theodorsen function C may give positive values of δ^*; moreover, since C is itself a function of the whirling frequency a more involved iterative procedure is needed to

solve for λ and $\bar{\zeta}$. In figure 7b only arbitrary values of δ^* are used to bring out the effect of the sign of δ^*. In the actual calculation of δ^* if $\omega_2 << \Omega$ is indicated, then $k \cong \Omega c/2W_\infty$ can be used for $\bar{F}$ and $\bar{G}$.

Finally, the importance of other competing mechanisms can be assessed. For example, the equivalent tangential force contributions to represent the effects of tip-clearance and load-input torque misalignment were added to C_{y_θ}. Both these mechanisms being absent for a non-lifting cascade, in reference 9 we have recalculated the R.S.D.'s and the torque coefficient for an assumed case of $\delta_o = 5°$. The resultant stability plot is shown in figure 7d with e/R as parameter. This plot demonstrates the possibility of forward whirl for certain values of e/R and also shows that backward whirl can be suppressed. According to refs. (3) and (5) both these load-dependent mechanisms give rise to forward whirl for aft-pivoted compressors. In our example, unless modified by the wake effect, only backward whirl is possible. The unsteady rotor wake effect depends on the sign of δ^* and no conclusion is possible pending additional investigation. The direction of whirling which is observed in a practical turbo-rotor is the resultant of all the mechanisms. Since $\bar{\zeta} \propto |b_o|$, it seems evident that an astute aerodynamic design should aim at making b_o small, thus leading to the total elimination of any undesirable whirl.

CONCLUSIONS

1. The propeller-whirl analogy can be directly applied to the whirl of axial turbo-machinery rotors with modifications for the cascade configuration. The basic driving mechanism of orthogonal moments is seen to remain the same.

2. A set of rotor stability derivatives (R.S.D.'s) for turbo-machinery rotors has been suggested. They are fundamental to the dynamic behavior. Expressions specifically derived for the coning mode of an aft-pivoted compressor with equivalent flat-plate, high solidity cascade are given. For practical applications, experimental verification of the expressions would be invaluable.

3. Quick survey of the dynamic stability as affected by various parameters is made possible by introducing artificial damping for neutral stability.

4. Considerations based on the R.S.D.'s suggest only backward whirl of compressors and turbines. The role of unsteady rotor wake is outlined but the net effect awaits more analysis.

5. The dynamic stability boundary plots reveal that stability can be increased by reducing the blade stagger, mass flow rate, density and increasing the stiffness of the shaft and external damping. Though an increase in overhang-to-tip radius ratio increases stability, the effective stiffness is decreased. Hence, an optimum e/R can be found.

6. Various mechanisms can be mutually annihilated by making the whirling group b_o as small as possible. This goal may be achievable at the preliminary design stage or later by modification of the rotor geometry, flow distribution or the structural properties.

ACKNOWLEDGEMENT

The basic idea of a closer examination of the aerodynamic forces and their role in whirl instability resulted from a discussion with Dr. F. F. Ehrich after his colloquium lecture at the Sibley School of Mechanical and Aerospace Engineering, Cornell University, in 1976. Dr. Ehrich's continued interest and constant encouragement have been essential in our progress to this date. Most of the work by the junior author (V.G.M.) was performed while holding a McMullen Fellowship.

REFERENCES

1. Ehrich, F. F.: Self-Excited Vibration. Shock and Vibration Handbook, McGraw-Hill, 1976, Chapter 5.

2. Shapiro, W. and Colsher, R.: Rotor Whirl in Turbo-machinery: Mechanisms, Analysis and Solution Approaches. ASME Winter Annual Meeting, Turbo-machinery developments in steam and gas turbines, N.Y., 1977, pp. 89-98.

3. Alford, J. S.: Protecting Turbo-machinery from Self-excited Rotor Whirl. J. Eng'g. for Power, ASME Trans., October 1965, pp. 333-344.

4. Pollman, E., Schwerdtfeger, H., and Termuehlen, H.: Flow-excited Vibration in High Pressure Turbines (steam-whirl). ASME Winter Annual Meeting, N.Y., 1977, pp. 75-87.

5. Bousso, D.: A stability criterion for rotating shafts. Israel J. of Technology, Vol. 10.6, 1972, pp. 409-423.

6. Vance, J. M.: Torque-whirl — A Theory to Explain Non-synchronous Whirling Failures of Rotors with High Speed and Load Torque. J. Eng'g. for Power, ASME, Vol. 100, April 1978, pp. 235-240.

7. Trent, R. and Lull, W. R.: Design and Control of Dynamic Behavior of Rotating Machinery. ASME Paper No. 72-DE-39, May 1972.

8. Ehrich, F. F.: An Aeroelastic Whirl Phenomenon in Turbo-machinery Rotors. ASME Paper No. 73-DET-97, 1973.

9. Mengle, V. G.: Non-synchronous Whirl in Axial Turbo-machinery Rotors Due to Fluid Dynamic Excitation. M.S. Thesis, Cornell University, August 1979.

10. Houbolt, J. C. and Reed, W. H.,III: Propeller Nacelle Whirl Flutter. J. Aero. Sc., Vol. 29. March 1962, pp. 333-346.

11. Reed, W. H., III and Bland, S. R.: An Analytical Treatment of Aircraft Propeller Precession Instability. N.A.S.A. Technical Note, TN D-659, Jan. 1961.

12. Hawthorne, W. R. (editor): Aerodynamics of Turbines and Compressors, High Speed Aerodynamics and Jet Propulsion. Vol. X, Princeton University Press, New Jersey, 1964, Section B.

13. Ribner, H. S.: Propeller in Yaw. N.A.C.A. Report No. 820, 1945.

14. Whitehead, D. S.: Force and Moment Coefficients for Vibrating Airfoils in Cascade. ARC, R & M No. 3254, London, 1962.

TABLE I.- TYPICAL VALUES USED FOR NUMERICAL ANALYSIS

Mass of the rotor	M = 21.89 kg (1.5 slugs)
Radius of tip of the rotor	R = 0.305 m (1 foot)
Hub-to-tip radius ratio	η_o = 0.75
Polar radius of gyration-to-tip radius ratio of the rotor	r_1/R = 0.6
Radius of gyration of the diametrical moment of inertia-to-tip radius ratio	r_2/R = 0.55
Standard density of air	ρ_o = 1.225 kg/m^3 (0.002378 slugs/ft^3)
Shaft overhang-to-tip radius ratio*	e/R = 0.3

*In figures 7c and 7d, e/R is a parameter.

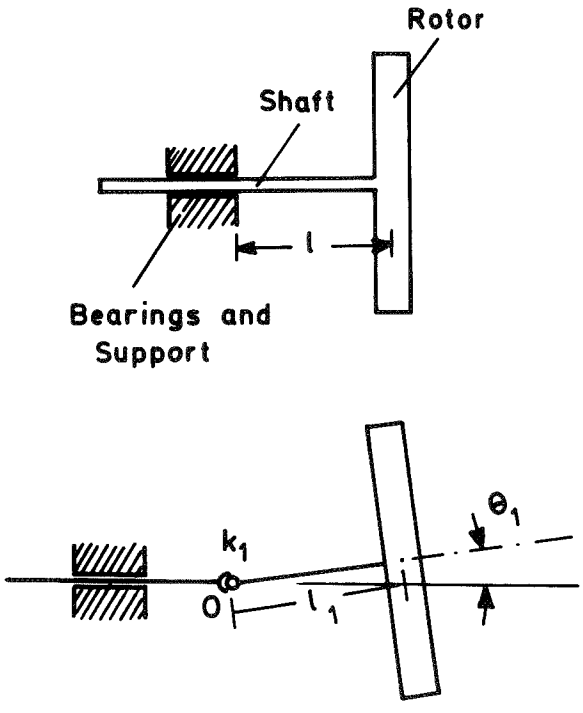

Figure 1. The rotor model.

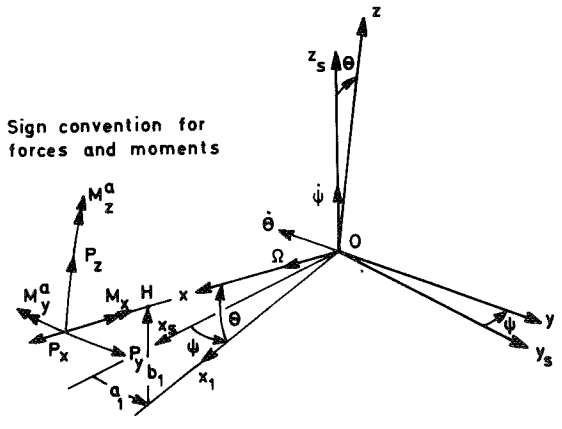

Figure 2. The reference frames and generalized coordinates.

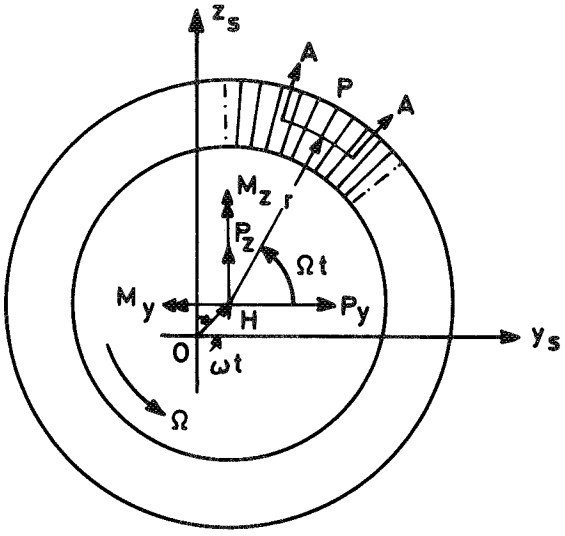

Figure 3a. The displaced rotor (front-view).

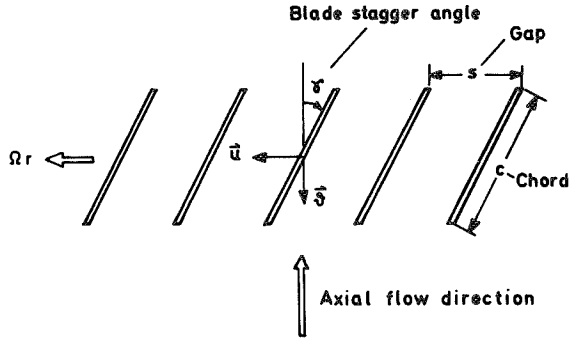

Figure 3b. The cascade nomenclature.

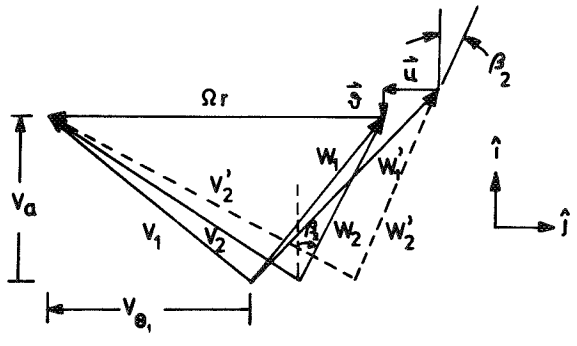

Figure 3c. The velocity triangles.

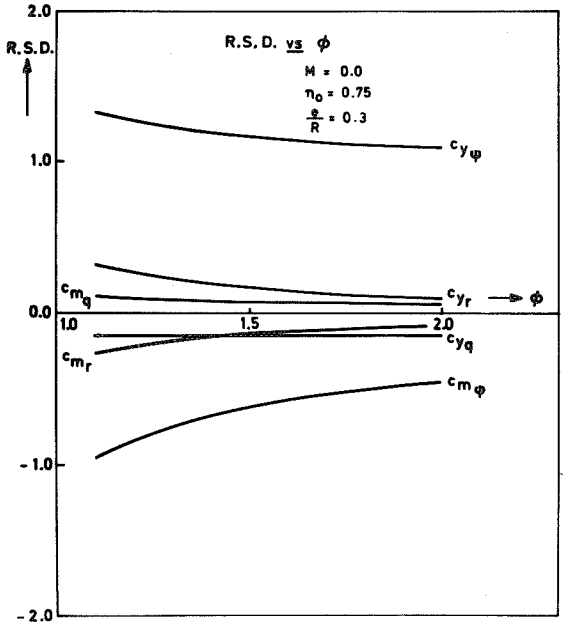

Figure 4. The rotor stability derivatives as functions of the mass-flow coefficient.

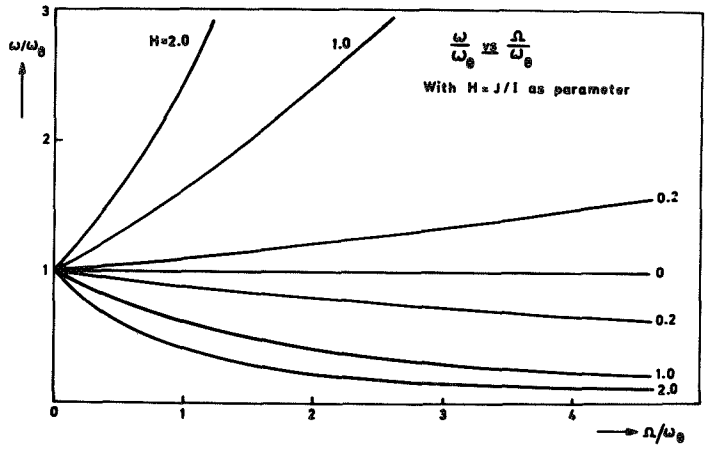

Figure 5. The natural whirling frequencies.

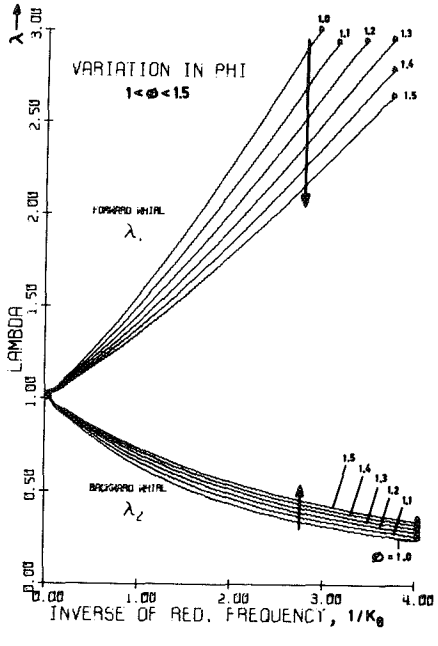

Figure 6. The forced whirling frequencies with mass-flow coefficient as parameter.

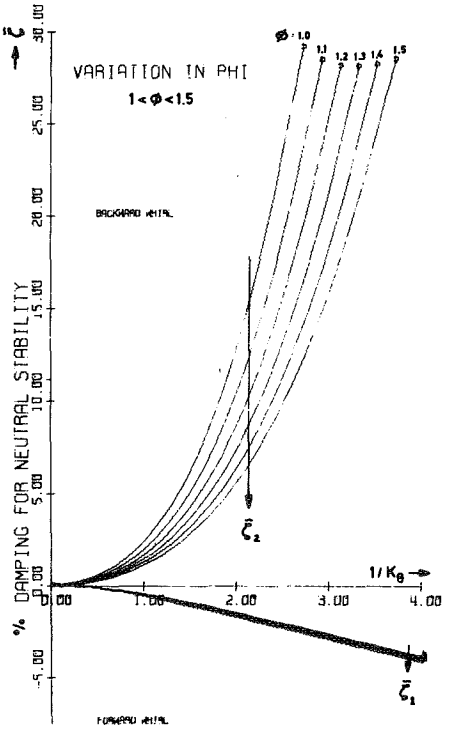

Figure 7a. Stability boundaries with mass-flow coefficient as parameter.

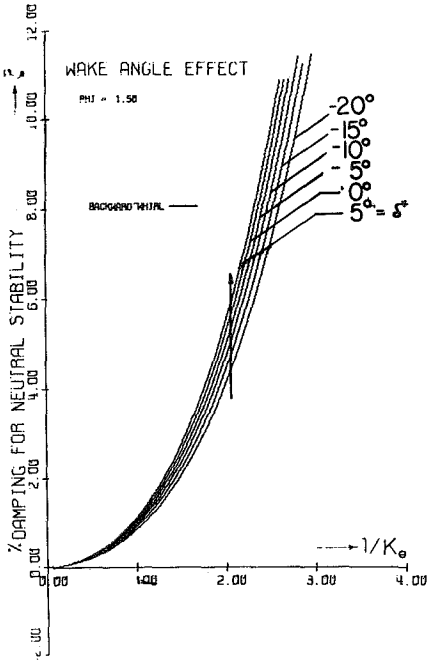

Figure 7b. Effect of wake-angle on the stability boundary.

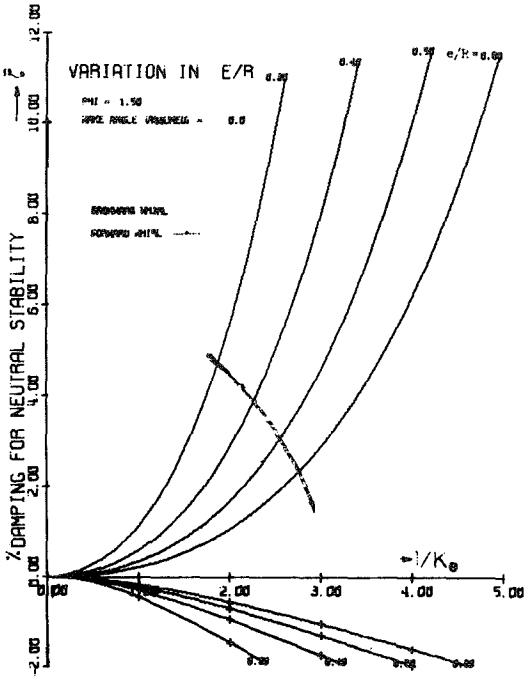

Figure 7c. Effect of shaft-overhang length on the stability boundary.

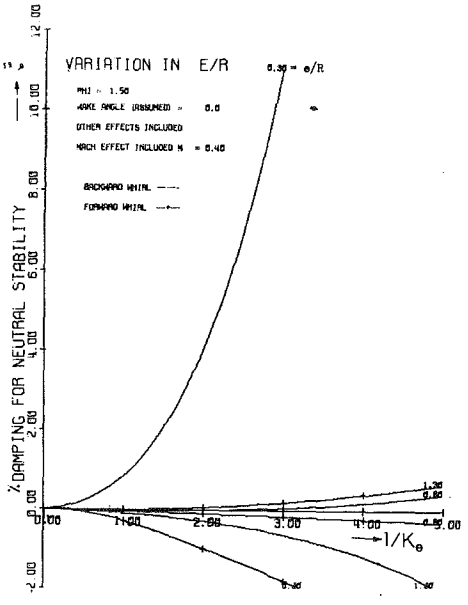

Figure 7d. Inclusion of other effects on the stability boundary with overhang shaft length as parameter.